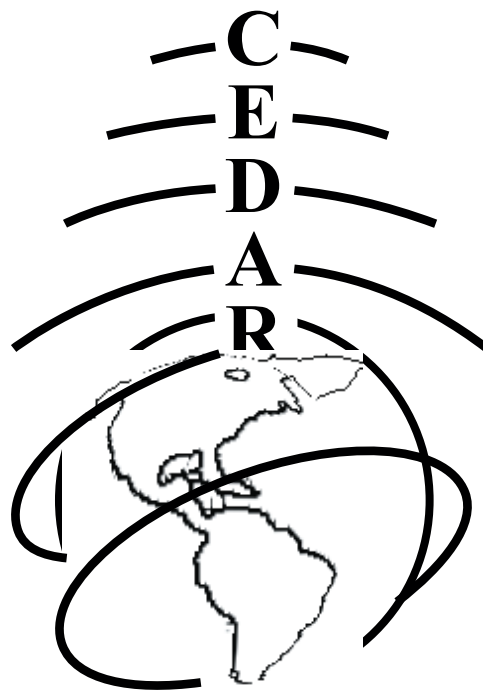


2007 CEDAR - DASI Workshop
Eldorado Hotel
Santa Fe, New Mexico, USA
June 24 - 29, 2007



Monday CEDAR Poster Session Booklet
June 25



Table of Contents

I. Equatorial Ionosphere or Thermosphere

| | |
|-----------------------------------------------------------------------------------------------------------------------------------------------------------|---|
| EQU-01, Matthew A. Hei, Stormtime Equatorial Electrodynamics: The Superfountain Effect..... | 1 |
| EQU-02, Patrick Alken, Spatio-temporal characterization of the equatorial electrojet from CHAMP, Oersted, and SAC-C satellite magnetic measurements | 1 |
| EQU-03, Tzu-Wei Fang, Equinoctical Asymmetry of the Vertical Drift in Pre-reversal Enhancement | 1 |
| EQU-04, Narayan P. Chapagain, Studies of Early Night Equatorial Spread F Over Jicamarca | 2 |
| EQU-05, Edgardo E. Pacheco, Latitude/Apex height Variations in the Ion Vertical Drift observed by ROCSAT-1 | 2 |
| EQU-06, Ronald Ilma, Jicamarca observations during November 2004 superstorm..... | 2 |
| EQU-07, Trevor Garner, Observations of the Equatorial Anomaly Peaks using the COSMIC Radio Beacon | 2 |

II. Long-Term Variations of Upper Atmosphere

| | |
|------------------------------------------------------------------------------------------------------------------------------------------------------------------|---|
| LTV-01, Yong Ha Kim – presented by Geonhwa Jee, Preliminary analysis of the observations from the Meteor Radar installed at King Sejong Station, Antarctica..... | 3 |
| LTV-02, Susan Marcelle Nossal, Geocoronal Hydrogen Observations from Three Solar Minimums..... | 3 |

III. Midlatitude Ionosphere or Thermosphere

| | |
|---------------------------------------------------------------------------------------------------------------------------------------------|---|
| MID-01, David J. Pawlowski, Global Model Comparisons with Millstone Hill | 3 |
| MID-02, Preeti Bhaneja, Midlatitude Spread F..... | 4 |
| MID-03, Edwin J Mierkiewicz, Geocoronal hydrogen Balmer alpha and Balmer beta observations obtained with WHAM..... | 4 |
| MID-04, Lara Waldrop Photoelectron impact excitation of OI 844.6 nm emission observed from Arecibo Observatory..... | 4 |
| MID-05, Mariangel Fedrizzi, Sources of F-region height changes during geomagnetic storms..... | 5 |
| MID-06, Ja Soon Shim, Spatial Correlations of Day-to-Day Ionospheric Total Electron Content Variability Obtained from Ground-Based GPS..... | 5 |

IV. Solar Terrestrial Interactions in the Upper Atmosphere

| | |
|---------------------------------------------------------------------------------------------------------------------------------|---|
| STI-01, Barbara Emery, Seasonal and Solar Flux Variations in the Electron and Ion Auroral Inputs | 6 |
| STI-02, Michael Alexander Danielides, Effects of auroral precipitation on high-latitude ion upwelling..... | 6 |
| STI-03, Xiaohua Fang, Changing energetic ion precipitation patterns during sawtooth oscillations | 7 |
| STI-04, Shasha Zou, High-Time Resolution Dayside Convection Monitoring by Incoherent Scatter Radar and Sample Application | 7 |
| STI-05, Young-Sil Kwak, Dependence of the High-Latitude Thermospheric Density on the Interplanetary Magnetic Field..... | 7 |
| STI-06, Clara Narvaez, Case study of upper atmospheric neutral | 8 |
| STI-07, Yue Deng, Analysis of thermospheric response to magnetospheric inputs..... | 8 |

V. Data Management and Visualization

| | |
|------------------------------------------------------------------------------------------------|---|
| VIZ-01, Brian Jackel, Global Auroral Imaging Access | 8 |
| VIZ-02, Brandon Taylor, Detecting Subauroral Polarization Streams in DMSP Satellite Data | 8 |

VI. Mannucci: I-T from Space

| | |
|-----------------------------------------------------------------------------------------------------------------|---|
| MAN-01, Michi Nishioka, Temporal and spatial variations of plasma bubble studied with global GPS-TEC data | 9 |
| MAN-02, Richard Eastes, Global-scale Observations of the Limb and Disk (GOLD)..... | 9 |

VII. Polar Ionosphere

| | |
|---------------------------------------------------------------------------------------------------------------------------------|----|
| POI-01, Craig Heinselman, Poker Flat AMISR Observations during the first three months of the IPY | 10 |
| POI-02, Stephen Capozzi, Estimating Energy Flux in the Earth's Polar Ionosphere from Incoherent Scatter Radar Measurements..... | 10 |
| POI-03, Matthew Zettergren, The Aeronomy of Auroral Ion Upflow | 10 |
| POI-04, Robert G Michell, Ground-based observations of auroral downward-current region processes..... | 11 |

VIII. Meteor Science Other Than Wind

| | |
|-------------------------------------------------------------------------------------------------------------------------------------------------------------|----|
| MET-01, Stanley Briczinski, Size does matter – The effect of radar wavelength on meteor results from high latitude observations..... | 11 |
| MET-02, Akshay Malhotra, A Radio Science Perspective on Long Duration Meteor Trails..... | 11 |
| MET-03, Jonathan Fentzke, A semi-empirical model of the contribution from sporadic meteoroid sources on the meteor input function observed at Arecibo | 12 |
| MET-04, Elizabeth Bass, Evaluating Mass Estimates from HPLA Radar Observations..... | 12 |

IX. Planetary Studies

| | |
|------------------------------------------------------------------------------------------------|----|
| PLA-01, Michael R. Line, Velocity Resolved Observations of the Extended Lunar Sodium Tail..... | 12 |
|------------------------------------------------------------------------------------------------|----|

X. Irregularities of the Ionosphere/Thermosphere and Ionospheric Heating Experiments

| | |
|---------------------------------------------------------------------------------------------------------------------------------------------|----|
| IIR-01, Greg Twork, Implementation of a Fabry-Pérot Interferometer | 13 |
| IIR-02, Jeffrey Spaleta, Analysis of Ionospheric Reflections During High Power, Short RF Pulse Experiments Conducted at HIPAS, Alaska | 13 |
| IIR-03, Richard Todd Parris, Imaging with the SuperDARN HF radar on Kodiak Island | 13 |
| IIR-04, Gwendolyn R Bryson, Improving SuperDARN Spatial Resolution..... | 13 |
| IIR-05, Tatsuhiro Yokoyama, Three-Dimensional Simulation of Midlatitude Ionospheric Irregularities in Coupled E and F Regions..... | 14 |
| IIR-06, Carlos Martinis, Imaging studies of ionospheric irregularities in the American sector and conjugate observations..... | 14 |

XI. Ionospheric Gravity Waves

| | |
|---------------------------------------------------------------------------------------------------------|----|
| GWI-01, Dorey Joeseph Livneh, Omnipresent Quasi-Periodic Waves in the F-region? | 14 |
| GWI-02, Roger Hale Varney, Observations of Electric Fields Associated with Internal Gravity Waves | 15 |
| GWI-03, Ilgin Seker, Clues to the 3D Structure of MSTID Bands Using ISR and Allsky Imaging, | 15 |

XII. Instruments or Techniques for Ionospheric or Thermospheric Observation

| | |
|-------------------------------------------------------------------------------------------------------------------|----|
| ITI-01, Lin Li , Vacuum Calibrations of the Cold Cathode Gauges in HEX-2 Mission..... | 15 |
| ITI-02, Marcos Diaz Particle-In-Cell Simulation of the Incoherent Scatter Radar Spectrum..... | 16 |
| ITI-03, Jeffrey Klenzing, Modeling Plasma Interactions with Satellite-Borne Instrumentation..... | 16 |
| ITI-04, Chad G. Carlson, A 1083 nm lidar for observations of temperature in the upper thermosphere..... | 16 |
| ITI-05, Konstantinos Kalogerakis, Remote O(3P) Sensing by Ionospheric Excitation (ROSIE), | 17 |
| ITI-06, Feng Han, The influence of high-energy electron precipitation on the midlatitude nighttime D region | 17 |
| ITI-07, Fabiano S. Rodrigues, Improved electron density profile estimation at Jicamarca | 17 |
| ITI-08, Fabiano S. Rodrigues, Recent observations of the proton gyroresonance at Jicamarca | 18 |
| ITI-09, Bill Wright – presented by Nick Zobotin, Transmitting Antennas for Modern Ionosondes..... | 18 |

| | |
|------------------------------------------------------------------------------------------------------------------------------------------------|----|
| ITI-10, Nick Zobotin, Line-of-sight Doppler and vector velocity relationships for HF sounding in the equatorial ionosphere | 18 |
| ITI-11, Romina Nikoukar, Investigation of a new incoherent scatter coding technique for F-region observations at the Arecibo Observatory | 19 |
| ITI-12, Eliana Nossa, Focal Phased Array Prototype for the Arecibo Telescope | 19 |

XIII. New Instrumentation

| | |
|---------------------------------------------------------------------------------------------------------------------------------------|----|
| NEW-01, Zhen Zeng, Ionospheric annual variations observed by the COSMIC radio occultation technique and simulated by the TIEGCM | 19 |
| NEW-02, Christopher Watts, Reconstructing the Ionosphere for the Long Wavelength Array | 20 |
| NEW-03, Scott E. Palo, Drag and Atmospheric Neutral Density Explorer (D A N D E)..... | 20 |
| NEW-04, Zachary Berkowitz, ISIS multi-antenna operation and calibration..... | 20 |
| NEW-05, Matthew Sunderland, Optimizations for Digital Radar Receivers..... | 21 |
| NEW-06, Elizabeth Silvestre, Distributed Observatory in South America of Ionospheric Measurements and Current Status | 21 |

Equatorial Ionosphere or Thermosphere

EQU-01 Stormtime Equatorial Electrodynamics: The Superfountain Effect - by Matthew A Hei

Status of First Author: Non-student

Authors: Matthew A. Hei, Cesar E. Valladares

Abstract: Electric fields produced by geomagnetic storms frequently penetrate to equatorial latitudes. In particular, large increases in the eastward zonal electric field cause an intensification of the upward ExB plasma drift at the equator. As a result, the amplitude and latitude of Equatorial Ionization Anomaly (EIA) ionization crests increase dramatically; this phenomenon has been referred to as the “Superfountain Effect”. We compare ground-based TEC measurements of the stormtime EIA with model results. The TEC measurements were obtained from the LISN array of GPS receivers in South America. The LLIONS ionospheric model, driven by ionosonde-derived estimates of vertical ExB drifts, was utilized for the comparison.

EQU-02 Spatio-temporal characterization of the equatorial electrojet from CHAMP, Oersted, and SAC-C satellite magnetic measurements - by Patrick Alken

Status of First Author: Student IN poster competition Masters

Authors: Patrick Alken (patrick.alken@noaa.gov), Stefan Maus (stefan.maus@noaa.gov)

Abstract: The equatorial electrojet (EEJ) is an eastward electric current on the day-side, flowing in a narrow band along the dip equator in the ionospheric E-region. Recent magnetic observations from the CHAMP, Oersted, and SAC-C satellites, comprising more than 95,000 dip equator crossings from 1999 to 2006, have provided an unprecedented longitudinal coverage of the EEJ magnetic signature. We have used these data to construct an empirical model of the EEJ current climatological mean and day to day variability as a function of longitude, local time, season, and solar flux. Our model has been successfully verified against vertical drift data from the JULIA radar at Jicamarca. We have also used the EEJ observations to estimate the self-correlation of the EEJ, confirming short longitudinal correlation lengths of 15 degrees, and finding a temporal correlation length of 2.4 hours.

Our model's predictions of the eastward electric field and its standard deviation may provide useful input to various kinds of ionospheric simulations. Coefficients and software are available online at:
<http://models.geomag.us/EEJ.html> and <http://www.earthref.org>.

EQU-03 Equinoctial Asymmetry of the Vertical Drift in Pre-reversal Enhancement - by Tzu-Wei Fang

Status of First Author: Student IN poster competition PhD

Authors: T. W. Fang^{1,2}, A. D. Richmond², M. Hagan², T. Yokoyama³, J. Y. Liu¹

¹ Institute of Space Science, National Central University, Chung-Li, Taiwan

² High Altitude Observatory, National Center for Atmospheric Research, Boulder, CO, USA

³ Department of Earth and Atmospheric Sciences, Cornell University, Ithaca, NY, USA

Abstract: The height of the post-sunset equatorial F-layer, which is the most important parameter in controlling the generation or inhibition of equatorial spread F (ESF), is largely driven by the equatorial vertical plasma drift ($E \times B$) velocity. Occurrence of ESF in different longitudes shows asymmetry between March and September equinoxes especially during solar minimum years. The asymmetry is also simulated by using NCAR Thermosphere Ionosphere Electrodynamics General Circulation Model (TIEGCM). In order to investigate the phenomenon, we examine the lower thermospheric tidal forcing which is driven by the Global-Scale Wave Model (GSWM) in the TIEGCM during the pre-reversal enhancement (PRE) under high and low solar activity. The occurrence time and magnitude of maximum PRE vertical drift show high dependence on the magnitude and phase of migrating tides in both equinoxes under low solar activity condition ($F10.7=80$) but no significant effects under high solar activity ($F10.7=200$). These results suggest that the tidal effects from the lower thermosphere (E region) may contribute to ionospheric F region PRE vertical drift especially during low solar activity period.

EQU-04 Studies of Early Night Equatorial Spread F Over Jicamarca - by Narayan P Chapagain

Status of First Author: Student IN poster competition PhD

Authors: Narayan P. Chapagain, Bela G. Fejer, npchapagain@cc.usu.edu, bfejer@cc.usu.edu, Center for Atmospheric and Space Science Utah State University

Abstract: We use Jicamarca JULIA and incoherent radar observations from 1996 to 2006 to study the initial development of equatorial spread F over Jicamarca. We show that the times of initial spread F occurrence do not change with solar flux, but their altitudes strongly increase from solar minimum to solar maximum. The times of initial radar plumes decrease with increasing solar flux during equinox and December Solstice. We will also discuss the seasonal and solar flux dependent relationships between the vertical plasma drift velocity and radar plume development.

EQU-05 Latitude/Apex height Variations in the Ion Vertical Drift observed by ROCSAT-1 - by Edgardo E. Pacheco

Status of First Author: Student IN poster competition PhD

Authors: Edgardo Pacheco, R. A. Heelis, S.-Y. Su

Abstract: Our knowledge of latitude (apex height) variations in the ion drift at low and middle latitudes is limited by the spatial location of ground based radars and by the difficulty in interpreting satellite measurements. Here we describe efforts to determine these variations using data from the Ionospheric Plasma and Electrodynamics Instrument (IPEI) on board ROCSAT-1 taken during the period 2000-2003. Specifically we derive the velocity perpendicular to the magnetic meridian and show conjugate latitude (apex height) variations at different longitudes. These variations will be contrasted with observations from Jicamarca and expectations based on the behavior of dynamo winds.

EQU-06 Jicamarca observations during November 2004 superstorm - by Ronald Ilma

Status of First Author: Non-student Undergraduate

Authors: R. R. Ilma(1), J. L. Chau(1) and M. A. Milla(2)

(1)Jicamarca Radio Observatory, Geophysical Institute of Peru, Lima, Peru

(2)Department of Electrical and Computer Engineering, University of Illinois at Urbana-Champaign, Urbana, Illinois, USA

Abstract: We report on the incoherent scatter (IS) radar observations conducted at Jicamarca during the geomagnetic storm of November 2004. Doppler measurements of the F-region radar returns provided estimates of the vertical plasma drifts. In the afternoon of November 9, 2004, these measurements recorded upward and downward velocities as large as 120 m/s. These values are larger than typical equatorial drifts, which are about 40 m/s during quiet ionospheric conditions [Woodman, 1970]. In addition, applying the differential-phase technique described in Kudeki et al. [2003], we have inverted the IS data collected during the campaign and obtained F-region electron densities. These measurements are compared to another set of density estimates obtained from calibration of the IS power profiles using ionosonde values. This procedure is a common practice at other IS radar facilities. According to the observations, the large upward and downward plasma drifts of November 9 accompanied the formation of a "second" ionosphere ranging from the F2 region to topside altitudes.

EQU-07 Observations of the Equatorial Anomaly Peaks using the COSMIC Radio Beacon - by Trevor Garner

Status of First Author: Non-student

Authors: T Garner, T L Gaussiran II, Applied Research Labs.: Univ. of Texas (gauss@arlut.utexas.edu), D. Munton, Applied Research Labs.: Univ. of Texas (muntond@arlut.utexas.edu), P Bernhardt, Naval Research Laboratory (paul.bernhardt@nrl.navy.mil)

Abstract: This poster presents the initial observations of the equatorial anomaly peaks using the radio signals from the CERTO beacons on board the COSMIC satellites.

Long-Term Variations of Upper Atmosphere

LTV-01 Preliminary analysis of the observations from the Meteor Radar installed at King Sejong Station, Antarctica - by Yong Ha Kim – presented by Geonhwa Jee

Status of First Author: Non-student

Authors: Y.-H. Kim, J.-H. Kim, C.-S. Lee, G. Jee, B.-Y Lee

Abstract: A meteor radar was installed at King Sejong station (62°13'S, 58°47'W), Antarctica in March 2007 for real time observation of meteors. When a meteor enters the atmosphere it rapidly vaporizes leaving behind a trail of ionized gas along its path of travel. Meteor radar transmits VHF radio wave (33.2 MHz) with the power of 8 kw and detects reflected signals from the trail of the ionized gas with 5 coherent receiver channels at the same time. Altitude and direction of meteors are observed in near-real time by analysing amplitudes and phases of the signals detected on the receiving antennas. A preliminary result of the observations shows a very sensitive performance of the radar detecting about 1000 meteors for an hour, Through the continuous observations for 24 hours per day, it is measuring temporal and spacial distributions of meteors over the Antarctica. The resulting height distribution of meteors shows the Gaussian distribution between 70 km and 110 km with the peak altitude of about 90 km. These 24-hour continuous observations of meteors will produce a temporal statistical data set of meteors over the Antarctica, as a fundamental dataset for the meteor astronomy. Furthermore, continuous measurements of meteor signals will allow to compute neutral winds and temperature at altitudes of 70 ~ 110 km in the upper atmosphere by detecting directions and diffusion coefficient of the ionized gases, respectively. In particular, with the existing observations of the OH airglow emission at King Sejong station, these measurements of neutral winds can be utilized to study the propagation processes of the waves in the upper atmosphere. Also, temperature measurements from the meteor radar can be compared with the temperature measurements from the observations of the OH airglow emission, which will allow to perform a systematic study of temperature changes in the upper atmosphere over the Antarctica.

LTV-02 Geocoronal Hydrogen Observations from Three Solar Minimums - by Susan Marcelle Nossal

Status of First Author: Non-student

Authors: Nossal, S.M., University of Wisconsin - Dept. of Physics, Mierkiewicz, E.J., Univ. of Wisconsin - Dept. of Physics Roesler, F.L., Univ. of Wisconsin - Dept. of Physics, Haffner, L.M., Univ. of Wisconsin - Dept. of Astronomy, Reynolds, R.J., Univ. of Wisconsin - Dept. of Astronomy, Woodward, R.C. University of Wisconsin - Fond du Lac

Abstract: The 11-year solar cycle is a dominant source of natural variability in the upper atmosphere and its effect on hydrogen distributions and emissions must be understood to investigate possible signs of longer-term climatic trends. We present mid-latitude geocoronal hydrogen Balmer α observations from three solar minimum periods, 1985, 1997, and 2006. The 1997 and 2006 observations were taken with the Wisconsin H α Mapper Fabry-Perot, a ground-based CCD-annular summing instrument located at the Kitt Peak Observatory in Arizona. The 1985 observations were made with a similarly designed Fabry-Perot Interferometer utilizing photomultiplier detection and located in Wisconsin. WHAM has observed higher column emission intensities during solar maximum periods than during solar minimum conditions with the increase dependent upon viewing geometry. There is generally good agreement between solar minimum observations taken in 1985 from Wisconsin and in 1997 and 2006 from Kitt Peak, Arizona. However, to isolate any small differences between these data sets, more work is required to identify and reduce sources of uncertainty.

Midlatitude Ionosphere or Thermosphere

MID-01 Global Model Comparisons with Millstone Hill - by David J Pawlowski

Status of First Author: Student IN poster competition PhD

Authors: David Pawlowski and Aaron Ridley, University of Michigan

Abstract: Results from 1D and 3D GITM are compared with data from the Millstone Hill incoherent scatter radar during the September 2005 World Month. The results show that the model performs the best during quiet time, and that it is necessary to include global dynamics in order to accurately simulate the mid-latitude ionosphere during storm times.

MID-02 Midlatitude Spread F - by Preeti Bhaneja

Status of First Author: Student IN poster competition PhD

Authors: P. Bhaneja, G.D.Earle, R. Bishop, R. Conkright

Abstract: This research involves a case study of Midlatitude Spread F (MSF) at Wallops Island (37.8°N, 75.5°W) using ionosonde data. Software has been developed in MATLAB to detect the edges of the O-Mode traces, so that range and frequency spreading can be objectively identified.

Findings based on work carried out to date include:

- Determination of seasonal and solar cycle variation patterns.
- Marked differences between MSF occurrence and duration during solar minimum and solar maximum.
- Previously published claims of anticorrelation between MSF and duration and the F10.7 index may require revision.

MID-03 Geocoronal hydrogen Balmer alpha and Balmer beta observations obtained with WHAM - by Edwin J Mierkiewicz

Status of First Author: Non-student

Authors: E. J. Mierkiewicz, F. L. Roesler, S. M. Nossal, L. M. Haffner, M. Sahan, R. J. Reynolds, G. Madsen

Abstract: In this poster we will present a set of near-coincident geocoronal hydrogen Balmer alpha and Balmer beta observations obtained with the Wisconsin H alpha Mapper (WHAM) Farby-Perot.

The geocoronal Balmer alpha emission feature (656.3 nm) arises predominately from fluorescence of atomic hydrogen, excited by resonant absorption of solar Lyman beta photons. Because geocoronal hydrogen fluorescence is primarily solar excited, the altitude of the earth's shadow at the time of an observation can be used as a first order determination of the base of the observed column emission. The shadow altitude is defined as the radial distance at which the (ground-based) observer's line-of-site intersects the earth's terminator (in the case of Balmer alpha, the shadow of the Lyman beta "black region" at ~102 km due to O₂ screening). Atomic hydrogen abundances in the upper atmosphere are large enough that multiple scattering of solar Lyman beta photons into the planetary shadow can contribute significantly to the Balmer alpha intensities observed at night.

In contrast, the atmosphere is more optically thin at Lyman gamma, hence Balmer beta fluorescence (which is predominately excited by resonant absorption of solar Lyman gamma photons) will have less of a multiple scattering contribution to its total observed intensity than Balmer alpha. Further, absorption of Lyman gamma is dominated by strong N₂ photoabsorption, placing the Lyman gamma "black level" above 160 km (well above the peak in atomic hydrogen densities near 80 km). Hence, even though Balmer beta intensities are roughly an order of magnitude smaller than Balmer alpha, the single scattering component to this emission will be dominant.

We will examine how the observed geocoronal Balmer alpha and Balmer beta intensities change with respect to shadow altitude and viewing geometry. Measurements of the variation of both these emissions can be used to constrain thermospheric and exospheric atomic hydrogen densities and fluxes retrieved through forward-model analysis (e.g., using the RT code `lyao_rt` of Bishop, 1999).

MID-04 Photoelectron impact excitation of OI 844.6 nm emission observed from Arecibo Observatory - by Lara Waldrop

Status of First Author: Non-student

Authors: L. Waldrop (UIUC), R. Kerr (Arecibo Observatory), P. Richards (Univ. of Alabama at Huntsville)

Abstract: Photoelectron (PE) impact on thermospheric oxygen atoms is a major source of OI 844.6 nm emission excitation at mid-latitudes. However, historical discrepancies between observed twilight emission brightnesses and photoelectron (PE) model

predictions have not only prompted speculation regarding secondary sources of excitation but also precluded the use of observed brightness as a much-needed diagnostic of thermospheric O density. In an effort to improve understanding of the physical mechanisms responsible for its excitation, this paper presents new photometric measurements of twilight OI 844.6 nm emission brightness, together with calculations using the FLIP PE model, acquired from Arecibo Observatory under geomagnetically quiet conditions during three winter campaigns from 1999-2002. Winter is a particularly favorable season for twilight 844.6 nm observation in the northern hemisphere since significant PE production, and thus 844.6 nm excitation, persists for several hours in the fully-illuminated, geomagnetic conjugate hemisphere in the absence of any local thermospheric illumination which quickly increases the background of the signal. Precise measurements of ion and electron density by the Arecibo Incoherent Scatter Radar (ISR) are used to estimate the strength of brightness contributions from radiative recombination. The winter 844.6 nm brightness data are fully consistent with a dominant PE impact excitation source. However, the new data also confirm a previous report of excess early morning brightness at Arecibo with respect to PE models which use a tilted-dipole approximation to the geomagnetic field. By using the IGRF geomagnetic field model to refine Arecibo's conjugate point location specified in the FLIP PE model, we demonstrate significantly improved agreement between the modeled and observed brightness decay profiles during both morning and evening twilight intervals. This simple geometric resolution to a long-standing discrepancy between 844.6 nm data and forward model calculations is an important step toward the reality of mid-latitude thermospheric remote sensing using twilight 844.6 nm measurements.

MID-05 Sources of F-region height changes during geomagnetic storms - by Mariangel Fedrizzi

Status of First Author: Non-student PhD

Authors: M. Fedrizzi (NOAA/SEC-CIRES/University of Colorado, e-mail: Mariangel.Fedrizzi@noaa.gov), T. J. Fuller-Rowell (NOAA/SEC-CIRES/University of Colorado, e-mail: Tim.Fuller-Rowell@noaa.gov), M. Codrescu (NOAA/SEC, e-mail: Mihail.Codrescu@noaa.gov), H. Khalsa (CIRES/University of Colorado, e-mail: Hargobind.Khalsa@noaa.gov)

Abstract: The increased high-latitude energy input during geomagnetic storms, mainly resulting from Joule heating, causes the atmosphere to heat and expand at thermospheric heights. As a consequence, a global wind surge is generated and propagates from both polar regions to low latitudes and into the opposite hemisphere. Those winds are driven by the pressure inequalities due to temperature differences between high and equatorial regions. Divergence in horizontal winds drive vertical upward winds across pressure surfaces, the so-called "divergence velocity" (W/D). Conversely, convergent horizontal winds are associated with a downward "divergence wind". The circulation is closed by a return flow in the lower thermosphere. At the same time, the expansion and contraction of a fixed pressure level atmospheric parcel cause vertical winds, the so-called "barometric velocity" (W/B). Barometric winds are related to the thermal expansion of the atmosphere, while vertical divergence winds are associated to the conservation of mass relative to the levels of fixed pressure. In this study, the relative contribution of the horizontal thermospheric winds, the divergence winds and the barometric winds in the thermosphere-ionosphere response to geomagnetic storms is examined and analysed using the global, three-dimensional, time-dependent, non-linear coupled model of the thermosphere, ionosphere, plasmasphere, and electrodynamics (CTIpe). Ionosonde data from various mid-latitude stations are used to compare and support results provided by the physical model.

MID-06 Spatial Correlations of Day-to-Day Ionospheric Total Electron Content Variability Obtained from Ground-Based GPS - by Ja Soon Shim

Status of First Author: Student IN poster competition PhD

Authors: J. S. Shim(jsshim@cc.usu.edu), L. Scherliess,(ludger@gaim.cass.usu.edu), R.W. Schunk(schunk@cc.usu.edu), D.C. Thompson(thompson@gaim.cass.usu.edu), Center for Atmospheric and Space Sciences, Utah State University, Logan, Utah

Abstract: We have studied the spatial correlations of day-to-day ionospheric total electron content (TEC) variations over a period of 4 months in 2004 (January, March/April, June/July, September/October) using more than 1000 ground-based GPS receivers. The spatial correlations were obtained in a 2-step process. Initially, the day-to-day variability was calculated by first mapping the observed slant TEC values for each 5-minute GPS ground receivers-satellite pair to the vertical using a simple geometrical factor and then differencing it with its corresponding value from the previous day. This resulted in more than 150 million values of day-to-day change in TEC (delta TEC). Next, statistic was performed on the delta TEC values to obtain their spatial correlations. Our study indicates strong correlations between geomagnetic conjugate points and these correlations are larger at low latitudes ($r = 0.62-0.73$) than at mid-latitudes ($r = 0.31-0.43$). Typical correlation lengths, defined as the length at which the correlation coefficient drops to 0.7, were found to be larger at mid-latitudes than at low latitudes. The meridian correlation lengths are about 10 degrees and 5 degrees at middle and low latitudes, respectively. The zonal correlation lengths are approximately 20 degrees at

mid-latitudes and 10 degrees at low latitudes. The correlation lengths are larger during daytime (1100-1300LT) than during nighttime (2300-0100LT). Our results indicate that the spatial correlation is largely independent of season. The local time and latitude dependence of the spatial correlation coefficients will be discussed.

Solar Terrestrial Interactions in the Upper Atmosphere

STI-01 Seasonal and Solar Flux Variations in the Electron and Ion Auroral Inputs - by Barbara Emery

Status of First Author: Non-student

Authors: Barbara A. Emery (HAO/NCAR, emery@ucar.edu), David S. Evans (SEC/NOAA, david.s.evans@noaa.gov), Frederick J. Rich (AFRL, frederick.rich@hanscom.af.mil), Glynn A. Germany (University of Alabama/Huntsville, germanyg@cspar.uah.edu), and Valerie Coumans (University of Liege, Belgium, v.coumans@ulg.ac.be)

Abstract: Models for electron and ion auroral energy inputs usually ignore seasonal or interhemispheric variations. Our study shows, however, that there are significant seasonal variations in the electron and ion auroral energy inputs, which are opposite to each other. The electron energy inputs were represented by hourly estimates of the electron hemispheric power (Hpe) (1) over 28 years from 24 intercalibrated NOAA and DMSP satellites, and (2) in the northern hemisphere (NH) over 1997-1999 during solar minimum from the UVI imager on the POLAR satellite. The ion hemispheric power (Hpi) was estimated (1) from four NOAA SEM-2 satellites over eight years, and (2) in the NH over two seasons in solar maximum from the FUV experiment on IMAGE. Annual cosines that peak at the solstices were fit to the NOAA/DMSP interhemispheric data binned according to the magnitude of Hpe and Hpi in the southern hemisphere (SH) and ordered in solar flux. Additionally, four-month seasonal averages were found for all the data as a function of Kp. The summer Hpe exceeded the winter Hpe by ~20% for Kp 0 and by nearly 30% for the lowest Hpe levels at low solar fluxes. For Hpe >~25 GW, the solstice winter Hpe exceeded the summer solstice Hpe by ~25%. The four-month winter excess Hpe was ~15% for Kp 3-5 for UVI and NOAA/DMSP. The summer Hpi was larger than the winter Hpi for all Hpi magnitudes by ~20%. The Hpi seasonal solar flux dependence was not clear using annual cosines, but the four-month average summer over winter increase was 18% for solar flux values <130 and 35% (double) for solar flux values >130. The summer to winter Hpi enhancement from IMAGE was similar at ~36%. Hpe decreased ~10% between solar flux 75 and 200 for all seasons at most Kps. The four-month summer Hpi increased 30% or more with increasing solar flux for all Kps, but the four-month winter Hpi remained approximately the same over the solar flux range. The annual seasonal variations were modeled as a function of Hp (e or i) magnitude, where the Hpe seasonal variation also depended explicitly on solar flux. The modeled seasonal variation can be added to the polynomial fits found for Hpe and Hpi as a function of Kp for use in models.

STI-02 Effects of auroral precipitation on high-latitude ion upwelling - by Michael Alexander Danielides

Status of First Author: Non-student PhD

Authors: M.A. Danielides, D. Lummerzheim, and A. Otto. All authors @ Geophysical Institute, University of Alaska Fairbanks, 903 Koyukuk Drive. P.O. Box 757320, Fairbanks, AK 99775-7320

Abstract: This presentation examines the generation, structure, and dynamics of vertical ion upwelling related to auroral precipitation. We use a 2-D three fluid ionospheric-magnetospheric coupling code to study a parameterization of auroral precipitation. Specifically we examine the effects of characteristic energy, energy flux, and heat conduction to study plasma pressure gradients and ion upwelling at different vertical and horizontal scales. The model enables us to compute the total plasma outflow and other plasma parameters with high horizontal and vertical resolution. Model results are also averaged to compare the plasma outflow seen by instrument resolution, e.g. EISCAT measurements compared to total plasma outflow. The parameterization of the auroral precipitation shall provide more insights to the sources of plasma pressure gradient increases.

Model results and observations show that soft auroral precipitating electrons (≈ 1 keV) are effective in rapidly enhancing the F-region ionization and electron temperature, which leads to a strong upward plasma expansion. A goal of this study is to demonstrate that soft electron precipitation is, in absence of frictional ion heating, the principal driver for a plasma pressure gradient increase in the topside F-region with large vertical plasma velocities (≈ 1500 m/s) at heights above 1000 km. The presentation of the parameterization analysis shows varying auroral precipitation directly impacting the vertical plasma velocity.

STI-03 Changing energetic ion precipitation patterns during sawtooth oscillations - by Xiaohua Fang

Status of First Author: Non-student

Authors: Xiaohua Fang, Janet Kozyra, Michael Liemohn, Xia Cai, David Evans, Howard Singer, Robert McPherron, Michelle Thomsen, and Michael Henderson

Abstract: Recently discovered “sawtooth oscillations” in the inner magnetosphere are an as yet poorly understood phenomena in which the magnetic field goes through a series of quasi-periodic stretching and dipolarizing intervals over a broad range of local times accompanied by nearly dispersionless high-energy particle injections at the geosynchronous altitude. Energetic ring current ion (>30 keV) precipitation into the upper atmosphere is examined in a number of carefully selected sawtooth oscillation events, in which the solar wind driving conditions are similar and relatively steady. The ion precipitation measurements by the NOAA/POES satellites are organized according to the stretching or dipolarization phase of each sawtooth oscillation, and then superposed together for all the storm events to achieve the global precipitation patterns. It is found that the stretching phase has a significantly different pattern on the ion precipitation than the dipolarization phase. While the patterns in both phases are characterized by a C-shaped morphology with a trough in the prenoon sector, the ion precipitation in the stretching phase is more symmetric. Within the main precipitation ovals, the stretching phase is associated with a larger amount of proton number fluxes than the dipolarization phase. However, along the equatorward edge in the dusk sector, there is clearly more ion precipitation in the dipolarization phase. While the equatorward boundaries in the two phases are almost the same, the main precipitation oval in the stretching phase is significantly broadened by extending the poleward boundary to a higher latitude by up to around 2°. It is implied that the physical processes in the stretching and dipolarization phases of sawtooth oscillations significantly differ from each other.

STI-04 High-Time Resolution Dayside Convection Monitoring by Incoherent Scatter Radar and Sample Application - by Shasha Zou

Status of First Author: Student IN poster competition Masters

Authors: S. Zou, L. R. Lyons, Department of Atmospheric and Oceanic Sciences, University of California, Los Angeles, Los Angeles, CA 90034, USA, sha@atmos.ucla.edu; larry@atmos.ucla.edu, M. A. McCready, C. J. Heinselman, Center for Geospace Studies, SRI International, Menlo Park, CA 94025, USA

Abstract: Convection and its changes, driven by the solar wind, are related to geomagnetic disturbances such as substorms, dynamic pressure disturbances and convection bays. Furthermore, convection is theoretically related to the evolution of the Harang electric field reversal (or “discontinuity”), which has been related observationally and theoretically to these disturbances. Interplanetary measurements are generally used for studying and making associations of convection with disturbances. This is generally acceptable for statistical studies, but spatial structure and propagation timing errors due to the highly variable orientation of interplanetary structures create significant ambiguity for case studies and have prevented definitive understanding. Moreover, small but geoeffective structure in the solar wind may be missed by even multi-spacecraft observations. Direct observation of dayside convection with high time resolution offers a potential solution to this problem. In this paper, we demonstrate that Sondrestrom incoherent scatter radar (ISR) observations have the ability to accurately monitor the dayside convection with ~2.5 min temporal resolution. The observations clearly show the dayside convection responses to IMF Bz, By and solar wind dynamic pressure variations and thus shed new light on how the magnetosphere and ionosphere respond to different external driving. Then, we illustrate an application of this technique by showing how it can be applied to study substorm triggering. We plan to use this technique in the future to study the relationships between convection, other geomagnetic disturbances, and the Harang reversal, as well as to evaluate the preceding convection strength and duration and the convection changes that lead to substorm onset.

STI-05 Dependence of the High-Latitude Thermospheric Density on the Interplanetary Magnetic Field - by Young-Sil Kwak

Status of First Author: Non-student

Authors: Young-Sil Kwak(1), Arthur D. Richmond(1), Yue Deng(1), and Jeffrey M. Forbes(2)
(1) NCAR High Altitude Observatory, Boulder, CO, USA
(2) University of Colorado, Boulder, CO, USA

Abstract: The direction and strength of the interplanetary magnetic field (IMF) has a strong influence on the high-latitude ionospheric plasma convection and current, thereby influencing the high-latitude thermospheric wind and forcing on the wind.

Thus one can expect that thermospheric density driven by the high-latitude forcing should also vary with respect to the IMF. In this study, the high-latitude thermospheric total mass density at 400 km, derived from the high-accuracy accelerometer on board the Challenging Minisatellite Payload (CHAMP) spacecraft, is statistically analyzed in magnetic coordinates as function of the direction and strength of the IMF for December solstice and high solar activity conditions. Moreover, a comparison of the observed CHAMP density with that simulated by the National Center for Atmospheric Research Thermosphere-Ionosphere Electrodynamics General Circulation Model (NCAR TIE-GCM) coupled with a new quantitative empirical model of the high-latitude forcing on the thermosphere, is also performed. This numerical experiment using model simulations can provide insight into sources responsible for driving the thermospheric density.

STI-06 Case study of upper atmospheric neutral densities - by Clara Narvaez

Status of First Author: Student IN poster competition Undergraduate

Authors: Clara Narvaez, Carlos Martinis, Jeff Forbes, Sean Bruinsma, Michael Mendillo

Abstract: In situ observation of the upper atmospheric neutral densities by the STAR accelerometer on the CHAMP satellite are compared to the optical all-sky imaging data from the Arecibo Observatory in Puerto Rico. The 6300 Å airglow images that illustrate atmospheric structures, and the corresponding density measurements from STAR, are analyzed in order to see if a relationship exists between density changes and appearance of structures. This pilot study deals with 21 nights in 2004 and 2005.

STI-07 Analysis of thermospheric response to magnetospheric inputs - by Yue Deng

Status of First Author: Non-student PhD

Authors: Yue Deng, Astrid Maute and Arthur Richmond

Abstract: Analyzing DE-2 satellite data and fitting the data to analytic functions of the independent variables, a new quantitative empirical model of the high-latitude forcing of the thermosphere has been developed, including electric potential, magnetic potential and Poynting flux. Coupling this empirical model with NCAR-TIEGCM, the influence of the high-latitude energy inputs and energy distributions on the global thermospheric temperature, density, and composition has been investigated. First, the Joule heating calculated with the average electric field which is called “simple Joule heating” and the Poynting flux from the empirical model are compared to show the contribution of electric field and magnetic field variability to the Joule heating. The total energy of the Poynting flux is 40% larger than the integrated simple Joule heating. The neutral density in the Poynting flux case increases in the whole polar region compared with the simple Joule heating case, and the hemispheric average temperature increases by 50-85 K. Secondly, an inter-comparison among three different methods to distribute the Poynting flux in altitude has been conducted. The difference of the thermosphere response suggests that not only the total amount of energy input, but the way to distribute the energy are significant for the impact of magnetosphere on the thermosphere and ionosphere.

Data Management and Visualization

VIZ-01 Global Auroral Imaging Access - by Brian Jackel

Status of First Author: Non-student

Authors: Brian Jackel, Steve Marple, Emma Spanswick, Mikko Syrjuasuo, Eric Donovan

Abstract: GAIA provides quick access to summary data from satellite and ground-based instruments that sense auroral precipitation. A combination of client-side javascript and distributed databases allow data from multiple sources to be browsed easily and effectively.

VIZ-02 Detecting Subauroral Polarization Streams in DMSP Satellite Data - by Brandon Taylor

Status of First Author: Student NOT in poster competition Undergraduate

Authors: Brandon Taylor, Hien Vo - Arecibo - Hvo@naic.edu

Abstract: Subauroral Polarization Streams (SAPs) have been detected in mid-latitude regions in conjunction with geomagnetic storms. Unfortunately, most studies on SAPs have been limited to relatively small datasets. By developing an algorithm to automatically detect SAPs events in DMSP satellite data we hope to gain a better statistical understanding of SAPs. This poster discusses a automated method of searching for SAP events. We also present some general statistics from three years of satellite data.

Mannucci: I-T from Space

MAN-01 Temporal and spatial variations of plasma bubble studied with global GPS-TEC data - by Michi Nishioka

Status of First Author: Student IN poster competition Masters

Authors: M. Nishioka, A. Saito (Department of Geophysics, Graduate School of Science, Kyoto University), S.Fukao, M.Yamamoto (Research Institute for Sustainable Humanosphere, Kyoto University), Y. Otsuka, T.Tsugawa (Solar-Terrestrial Environment Laboratory, Nagoya University)

Abstract: Temporal and spatial variations of plasma bubble were studied using GPS total electron content (TEC) data. GPS data used in this study is provided by International GNSS Service, Scripps Orbit and Permanent Array Center, and Japan Agency for Marine-Earth Science and Technology. The receivers of these networks cover all longitudinal sectors and provide TEC data every 30 seconds.

Plasma bubble can be identified using the TEC data. Therefore the global picture of plasma bubble occurrence can be investigated for every day. In this presentation, (1) temporal variability of plasma bubble occurrence and (2) zonal distribution of plasma bubble will be discussed. (1) Yearly, monthly, several days and day-to-day variations were investigated from 2000 to 2006 in the five regions; the Asian, Central Pacific, Eastern Pacific, Atlantic and African regions. These variations were different among regions. (2) zonal distribution of plasma bubble was investigated in detail between 60E and 150E in 2003. Typical zonal width of plasma bubbles was 100km-200km. A few plasma bubbles appeared as a “plasma cluster”, which zonal width was 200-800km. Probability of its occurrence was 12%/50km on the average. There were 400km-scale sectors where the occurrence probabilities were 25%/50km and 5%/50km, respectively.

MAN-02 Global-scale Observations of the Limb and Disk (GOLD) - by Richard Eastes

Status of First Author: Non-student

Authors: R. Eastes, W. McClintock, A. Aksnes, D. Anderson, L. Andersson, A. Burns, S. Budzien, M. Codrescu, R. Daniell, K. Dymond, F. Eparvier, J. Harvey, T. Immel, A. Krywonos, M. Lankton, J. Lumpe, G. Pröls, A. Richmond, D. Rusch, S. Solomon, D. Strickland and T. Woods

Abstract: The Global-scale Observations of the Limb and Disk (GOLD) experiment is an ultraviolet imager being considered for flight on a geostationary (GEO) satellite as part of the upcoming Radiation Belt Storm Probes (RBSP) mission. On the daytime disk, high spectral resolution observations will give the first global-scale images of the neutral temperatures in the lower thermosphere (near 150 km). Limb measurements of atmospheric emissions and stellar occultations will provide complementary temperature data at higher altitudes, as well as a direct measurement of the thermospheric O₂ density profile. In addition, GOLD will perform more familiar measurements, such as the atomic oxygen to molecular nitrogen (O/N₂) ratio and night-time O⁺ density. From GEO, GOLD will almost continuously observe the same hemisphere and provide daily measurements at all local times. The simultaneous measurements of (O/N₂) and neutral temperature will enable advances in ionosphere-thermosphere modeling capabilities and allow us to understand: (1) the global-scale response of the thermosphere and ionosphere to geomagnetic and solar forcing; (2) the global-scale tidal amplitude and phase variations; and (3) the causes of small-scale ionospheric density irregularities. Simulations of observations by GOLD and retrievals of information from the simulated observations will be presented.

Polar Ionosphere

POI-01 Poker Flat AMISR Observations during the first three months of the IPY - by Craig Heinselman

Status of First Author: Non-student PhD

Authors: 1. Craig Heinselman, SRI International, craig.heinselman@sri.com
2. Michael Nicolls, SRI International, michael.nicolls@sri.com
3. Jan Sojka, Utah State University, fasojka@gaim.cass.usu.edu

Abstract: The Poker Flat Advanced Modular Incoherent Scatter Radar (AMISR) has been operating in a low-duty cycle, single look-direction (parallel to B) mode in support of the International Polar Year (IPY). The radar has been running in this mode continuously when not scheduled for user operations. The synoptic mode consists of 15-minute estimates of densities and temperatures throughout the E and F regions. Here we present summary plots of the first three months of observations, which consist of several long-duration, uninterrupted periods of observations. This dataset will be a useful tool for synoptic-scale modeling efforts and for day-to-day variability studies.

POI-02 Estimating Energy Flux in the Earth's Polar Ionosphere from Incoherent Scatter Radar Measurements - by Stephen Capozzi

Status of First Author: Student IN poster competition

Authors: Stephen Capozzi and Joshua Semeter

Abstract: Incoherent Scatter (IS) radar measurements of the polar upper atmosphere can be used to uncover the coupling between Electromagnetic (EM) energy flux and Kinetic energy (KE) flux in the earth's ionosphere-thermosphere (IT). This incoming energy flux originates from electrodynamic coupling between the solar wind and the magnetosphere. This energy is ultimately dissipated in the form of heat, ionization, and auroral excitation, in the Earth's ionosphere. We probe the ionosphere at two frequencies simultaneously, one with a coded pulse and one with an uncoded pulse. Coded IS radar pulses give high range resolution electron density. These measurements can be used to estimate KE flux via Maximum Entropy inversion (Semeter and Kamlabadi, 2005). Plasma parameters derived from the doppler spectrum of uncoded IS pulse measurements can be used to estimate the horizontal electric field magnitude and, hence, EM influx. Integrating KE and EM flux over altitude gives the total incoming energy flux for the ionospheric region of interest. The primary benefit of using ground-based radar measurements versus spacecraft measurements is the ability to monitor the coupling of KE flux and EM energy flux over space and time in the auroral zone.

POI-03 The Aeronomy of Auroral Ion Upflow - by Matthew Zettergren

Status of First Author: Student IN poster competition PhD

Authors: Matthew Zettergren , Joshua Semeter , Kristina Lynch , and Marcos Diaz

Abstract: The magnetosphere is populated with significant amounts of O⁺, which is commonly observed in the ring current, plasma sheet, and magnetospheric tail lobes. Since there is very little O⁺ in the solar wind these ions must originate from the high-latitude terrestrial ionosphere. A variety of physical mechanisms, including pressure gradients, transverse ion acceleration processes, and parallel electric fields, are responsible for transporting ions into the magnetosphere. Because these mechanisms operate over a enormous range of temporal and spatial scale sizes, different instruments are required to observe their micro- and macro-physical aspects. Incoherent scatter radar, sounding rockets, and satellites are widely used to study ion outflow. This work focuses on another, seldom used, diagnostic for ion outflow: auroral optical emissions.

Energy deposition by auroral particle precipitation is responsible for a variety of effects including electron production and heating, and atomic excitation and emission. Pressure-driven ion upflows are a secondary effect of the increased plasma density and temperature. Our goal is to use one effect of the particle precipitation (optical emissions) to study another effect (ion upflows). We take a modeling approach to determine how optical emissions can be used as a quantitative diagnostic for ion outflows. A kinetic model of electron energy deposition is used to determine optical emissions and electron heating, and a fluid approach is

used to capture the ionospheric response. These models (collectively known as TRANSCAR) allow us to construct an inverse technique for inferring ion upflow from optical measurements.

POI-04 Ground-based observations of auroral downward-current region processes - by Robert G Michell

Status of First Author: Student IN poster competition PhD

Authors: Robert Michell, Kristina Lynch, Hans Nielsen, Craig Heinselman

Abstract: This poster presents data from ground camera observations of the aurora conducted from Alaska during the winters of 2005 through 2007. In conjunction with these camera observations, conjugate radar observations of the auroral ionosphere were conducted during the winters of 2006 and 2007, using the Poker Flat Advanced Modular Incoherent Scatter Radar (AMISR). Two main aspects of auroral downward-current and Alfvénic / polar cap boundary regions are investigated, namely, black auroral signatures in the camera data, and naturally enhanced ion acoustic lines (NEIALs) in the radar data. An auroral event containing a distinct black stripe occurred on 06 March 2005 over Kaktovik, Alaska. This event displayed many characteristics of an auroral DCR, as compared to in situ studies of DCRs using data from the FAST and Cluster satellites. The second aspect of these auroral regions investigated here is the occurrence of NEIALs in the radar data. The occurrence of NEIALs is compared to the occurrence of broad-band extremely low frequency wave activity (BBELF) in situ. Observations of NEIALs are presented from two separate nights, displaying different auroral context. The focus here is to compare the optical observations to the morphology and auroral context of DCRs as measured in situ by previous studies. The use of ground-based observational techniques for observing DCR processes has many implications. These include identifying and following the temporal and spatial evolution of DCRs as well as being able to identify regions of potential ion outflow on a large spatial and temporal scale using ground based optical observations.

Meteor Science Other Than Wind

MET-01 Size does matter – The effect of radar wavelength on meteor results from high latitude observations - by Stanley Briczinski

Status of First Author: Student NOT in poster competition PhD

Authors: S.J. Briczinski, J.D. Mathews, C.J. Heinselman, D.D. Meisel

Abstract: While much progress has been made in understanding the radio science and meteor physics implications of the meteor “head-echo” observed with high power, large aperture (HPLA) radars, issues remain particularly regarding frequency and latitude dependency of the observed meteor altitude and speed distributions. We address these issues via the first ever use and analysis of meteor observations from AMISR Poker Flat (449.3 MHz), Sondrestrom (1290 MHz), and Arecibo (430 MHz) radars. The AMISR and Sondrestrom radars are located near the arctic circle while Arecibo is in the tropics. The meteors observed at each radar were detected and analyzed using the same automated FFT periodic micrometeor searching algorithm reported by Mathews et al [JASTP 65, 1139-1149 (2003)]. Sporadic meteor data were taken using the 1290 MHz Sondrestrom incoherent scatter radar and the 449.3 MHz Advanced Modular Incoherent Scatter Radar (AMISR) at the Poker Flat Research Range, Alaska. The automated search/analysis algorithm was run on the data sets from both radars and then compared to sporadic meteor observations taken at the 430 MHz radar at the Arecibo Observatory at similar dates in the calendar year. We present and compare sporadic meteor parameters (event altitude, velocity, and deceleration distributions) from all three facilities and in so doing observe a striking altitude “ceiling effect” in the 1290 MHz results relative to the 430/449.3 MHz results. This effect is even more striking in that the Arecibo and AMISR distributions are nearly identical even though the two radars are over 1000 times different in sensitivity and at very different latitudes. That is, the meteor altitude distribution comparisons provide the first statistical evidence that HPLA meteor radar observations are dominated by the incident wavelength, regardless of the other radar parameters.

MET-02 A Radio Science Perspective on Long Duration Meteor Trails - by Akshay Malhotra

Status of First Author: Student IN poster competition PhD

Authors: Akshay Malhotra, John Mathews, Julio Urbina

Abstract: Non-classical radar meteor echoes or range spread trail echoes (RSTEs), lasting from tens of seconds to over 15 minutes, have been a subject of considerable interest and speculation in the community ever since they were first observed in the 1940s. Using data collected from the Jicamarca Radio Observatory (JRO) 50 MHz radar (11.95° S, 76.87° W) in June 2006, we find that these long-duration echoes can be explained largely from a radio science perspective and are observed almost exclusively from scatterers in the k perpendicular to B region. We find the aspect sensitivity of evolving meteor trails to be the primary constraint for observing these long duration echoes. This conclusion has far-reaching implications to our current understanding of meteor physics including the time duration of most meteor trail echoes.

MET-03 A semi-empirical model of the contribution from sporadic meteoroid sources on the meteor input function observed at Arecibo - by Jonathan Fentzke

Status of First Author: Student IN poster competition PhD

Authors: Jonathan Fentzke, NorthWest Research Associates Inc., CoRA Division, 3380 Mitchell Lane, Boulder, CO 80301, USA
Department of Aerospace Engineering Sciences, University of Colorado, 429 UCB, Boulder CO 80309-0429, USA
jonathan.fentzke@colorado.edu; Diego Janches, NorthWest Research Associates Inc., CoRA Division, 3380 Mitchell Lane, Boulder, CO 80301, USA, diego@cora.nwra.com

Abstract: Microgram extraterrestrial particles from the sporadic background are widely believed to be the major contributors of metals in the Mesosphere/Lower Thermosphere (MLT). It is well established that this material gives rise to the upper atmospheric metallic and ion layers observed by radars and lidars. In addition, micrometeoroids are believed to be an important source for condensation nuclei (CN), a prerequisite for the formation of NLC particles in the polar mesopause region. In order to understand how this flux gives rise to these atmospheric phenomena, accurate knowledge of the global meteoric input function (MIF) is critical. In this work, we present results from a detailed model of the diurnal and seasonal variability of the micrometeoroid activity in the MLT as observed by the 430 MHz Arecibo radar. The model uses Monte Carlo simulation techniques and includes an accepted mass flux provided by six main known meteor sources (i.e. orbital families of dust) and a detailed modeling of the meteoroid atmospheric entry and ablation physics. The principal goal of this effort is to construct a more precise sporadic MIF needed for the subsequent modeling of the atmospheric chemistry of meteoric material and the origin and formation of metal layers in the MLT.

MET-04 Evaluating Mass Estimates from HPLA Radar Observations - by Elizabeth Bass

Status of First Author: Student IN poster competition PhD

Authors: Elizabeth Bass (enb@bu.edu), Boston University,, Meers Oppenheim (meerso@bu.edu), Boston University, Jorge Chau, Jicamarca Radio Observatory

Abstract: This poster evaluates the accuracy of meteor masses determined from meteor head echo data. This involved comparing actual data with models of what we would expect to observe. Simulations were used to determine the mass, temperature, and velocity of a meteoroid along its trajectory. After estimating the meteor ionization rate and radar reflection strength, noise was added to resemble our radar data. These expected signals were compared to high resolution meteor observations which were obtained in July 2005 using the 50MHz antenna at the Jicamarca Radio Observatory (JRO) in Peru. The meteor mass was then calculated using different algorithms for both the simulated and actual signals in order to determine which techniques are the most accurate.

Planetary Studies

PLA-01 Velocity Resolved Observations of the Extended Lunar Sodium Tail - by Michael R Line

Status of First Author: Student IN poster competition Undergraduate

Authors: M.R. Line, E.J. Mierkiewicz, F.L. Roesler, L.M. Haffner, R.J. Oliverson

Abstract: We present velocity resolved sodium D2 (5889.950 Å) line profile observations of the extended lunar sodium tail observed in the anti-lunar direction within 2-18 hours from new Moon. These observations were made in March, April, and September, 2006 and April, 2007 from Pine Bluff (WI) Observatory (PBO) with a double etalon Fabry Perot spectrometer. The

PBO Fabry-Perot is coupled to a siderostat with a circular 1.5 degree field-of-view on the sky, and samples a 75 km/s spectral interval with 3.5 km/s spectral resolution at 5890 Å.

The average observed radial velocity of the lunar sodium tail in the vicinity of the anti lunar point was 12 km/s from geocentric zero; the average Doppler width of a single Gaussian fit to the emission line was 8 km/s. We will present our current work, which involves mapping the spatial distribution of this emission over an 8 degree field on the sky.

This work is partially supported by the National Science Foundation through grants ATM-0228465 and ATM-0535433

Irregularities of the Ionosphere/Thermosphere and Ionospheric Heating Experiments

IIR-01 Implementation of a Fabry-Pérot Interferometer - by Greg Twork

Status of First Author: Student IN poster competition Undergraduate

Authors: Greg Twork, gtwork@clermson.edu, Dr. John Meriwether, john.meriwether@ces.clemson.edu

Abstract: The Pisgah Astronomical Research Institute (PARI) is a non-profit public foundation that collaborates with several universities, with the purpose of providing an educational and research opportunities in the many fields of science. In July, 2007, Clemson University will install a Fabry-Pérot interferometer at PARI, which will be used to study the upper atmosphere winds and temperatures by measuring the Doppler shifts and Doppler broadenings of the 630 nm emission of atomic oxygen. Once the installation is finished, the instrument will used both as an experimental station, and as an educational tool.

IIR-02 Analysis of Ionospheric Reflections During High Power, Short RF Pulse Experiments Conducted at HIPAS, Alaska - by Jeffrey Spaleta

Status of First Author: Non-student

Authors: J. Spaleta, A. Y. Wong, W. Wang, J. Hummel

Abstract: A series of experiments to investigate the ionospheric response to high power, short duration radio frequency pulses was conducted recently at the HIPAS ionospheric heating facility. A digital RF receiver located on-site at HIPAS was used to record both the transmitted groundwave pulse and the skywave return pulse reflected from the ionosphere. Of particular interest was the characterization the dependency of reflected skywave power on groundwave power. Presented here are the preliminary results for an experiment during stable F-region reflection using 2.85 MHz transmission pulses. The analysis shows a modest non-linear relationship between skywave return power and transmitted groundwave power, which is unrelated to observed time-varying fluctuations in skywave power due to local changes in ionospheric conditions.

IIR-03 Imaging with the SuperDARN HF radar on Kodiak Island - by Richard Todd Parris

Status of First Author: Student NOT in poster competition PhD

Authors: R. T. Parris, Geophysical Institute, University of Alaska Fairbanks, W. A. Bristow, Geophysical Institute, University of Alaska Fairbanks

Abstract: A new imaging receiver system is being developed for the SuperDARN radar on Kodiak Island. This new system will permit higher spatial resolution observations of the decameter scale field-aligned density irregularities in the E and F-regions of the Ionospher. The details and status of this new system will be presented.

IIR-04 Improving SuperDARN Spatial Resolution - by Gwendolyn R Bryson

Status of First Author: Student NOT in poster competition Masters

Authors: Gwendolyn R. Bryson, ftgrb@uaf.edu, Dr. William A. Bristow, bill.bristow@gi.alaska.edu

Abstract: The observation process of any radar is a convolution of the transmitted signal with a given target in space. This convolution smears out details of the target with a scale shorter than the length of the radar pulse. In order to recover information about a target's small-scale features, the returned signal must, therefore, be deconvolved. A recent experiment was run using the Kodiak SuperDARN radar and the HAARP Ionospheric Research Instrument to investigate the applicability of a deconvolution algorithm for the purpose of improving the spatial resolution of SuperDARN while investigating the evolution of the heated region over HAARP.

IIR-05 Three-Dimensional Simulation of Midlatitude Ionospheric Irregularities in Coupled E and F Regions - by Tatsuhiro Yokoyama

Status of First Author: Non-student

Authors: T. Yokoyama(1, 2), Y. Otsuka(2), and T. Ogawa(2), (1)Department of Earth and Atmospheric Sciences, Cornell University, USA, (2)Solar-Terrestrial Environment Laboratory, Nagoya University, Japan

Abstract: Since the discovery of turbulent upwelling associated with midlatitude spread F with the MU radar, midlatitude ionosphere has been intensively studied for the last two decades. Two-dimensional airglow images or GPS-TEC maps have revealed that banded structures, or medium-scale traveling ionospheric disturbances (TIDs) frequently occur in the nighttime midlatitude ionosphere. Although it is accepted that the Perkins instability is the most likely mechanism to explain the TID structures, the rapid growth and the southwestward propagation of the TID cannot be derived from the linear theory of the Perkins instability. Recently, it is proposed that the coupled electrodynamic between the E and F regions plays an important role in the growth of the Perkins instability. For the purpose of studying the coupled electrodynamic, we have employed three-dimensional numerical model which covers altitudes from 90 km to about 500 km. Growth of the Perkins instability is successfully reproduced with this model in the typical nighttime condition, while the instability does not grow under the condition that a uniform sporadic-E (Es) layer exists in the coupled E region. On the other hand, the polarization electric field generated in a modulated Es layer can map up to the F region and effectively seed the Perkins instability. The coupled electrodynamic is essential for understanding the phenomena in the midlatitude E and F regions.

IIR-06 Imaging studies of ionospheric irregularities in the American sector and conjugate observations - by Carlos Martinis

Status of First Author: Non-student PhD

Authors: C. Martinis, martinis@bu.edu, J. Baumgardner, jeffreymb@bu.edu, M. Mendillo, mendillo@bu.edu

Abstract: All-sky imagers located at Arecibo, Puerto Rico (18.3o N, 66.7o W, 28o N mag lat) and El Leoncito, Argentina (31.8o S, 69.3o W, 18o S mag lat), are used to compare 630.0 nm airglow emission features. Typical mid-latitude processes related to Perkins instability are common features observed at Arecibo, but not at El Leoncito, where Rayleigh-Taylor instability processes are the dominant feature. Two case studies (2 Nov 2002 and 26 Feb 2003) show the occurrence of simultaneous airglow depletions associated with equatorial spread-F. Supporting information is obtained from DMSP, ROCSAT-1 and GPS data, all of them showing the presence of strong ionospheric irregularities collocated with the airglow depletions. Typical mid-latitude airglow bands have also been observed at El Leoncito. Thus, the region poleward of ~18 magnetic latitude and equatorward of ~28 magnetic latitude is a good example of a transition region in which low latitude processes can extend to midlatitudes and vice versa.

Ionospheric Gravity Waves

GWI-01 Omnipresent Quasi-Periodic Waves in the F-region? - by Dorey Joseph Livneh

Status of First Author: Student IN poster competition PhD

Authors: Dorey J. Livneh, PSU, John D. Mathews, PSU, Frank T. Djuth, Geospace Research Inc., Ilgin Seker, PSU

Abstract: Incoherent Scatter Radar power profile observations at Arecibo and Millstone Hill Observatories have revealed the continuous presence of long vertical wavelength (>100 km) quasi-coherent waves with periods of ~55 minutes. The waves were observed to be nearly continuously present over four multi-day geomagnetically quiet observation periods at Arecibo and a full month period of varying geomagnetic activity at Millstone Hill. Upon filtering, the waves were seen unambiguously and

ubiquitously in Arecibo results from 22-23 March 2004, and 5-6 June, 21-25 September, and 17-20 November 2005, as well as Millstone Hill results from 4 October to 4 November, 2002. The waves are strong throughout the F-region, often spanning 160 km to above 500 km in altitude, and are detected day and night in the F2-layer. In fact, the waves are seen at every time and altitude that there is sufficient plasma to detect them. The consistent detection of the waves, along with the large spread of the observation sites suggests that these waves are always present over at least eastern North America. Airglow imager results at Arecibo indicate a southwestern direction of travel for the waves. While traveling-ionospheric disturbances (TIDs) are traditionally associated with acoustic-gravity waves (AGWs), this may or may not be the case for these waves because of their continuous presence through a range of geographical locations and altitudes. Further observations will help construct a more complete understanding of the extent of the phenomenon.

GWI-02 Observations of Electric Fields Associated with Internal Gravity Waves - by Roger Hale Varney

Status of First Author: Student IN poster competition Undergraduate

Authors: Roger Varney, Michael Kelley, Erhan Kudeki

Abstract: Measurements of the ion drift perpendicular to the magnetic field allow an unambiguous determination of the electric field in that plane. At the Jicamarca Radio Observatory the vertical drift component yields a very accurate measure of the eastward electric field since the spectrum of the ISR signal is extremely narrow in the plane perpendicular to B. Occasionally this drift component displays a downward-phase progression, which is evidence for a relationship to a gravity wave. The idea that gravity waves can create electric fields has been around for awhile but there are only two cases reported in the literature, one being from the same data set discussed here. We examined the Jicamarca database for events of this type and made an attempt to determine the properties of the associated waves. The only measurables we have are the amplitudes, the frequency in the earth-fixed frame and the vertical wavelength. We extend the information as follows. In order to avoid shorting by the current along magnetic field lines, we argue that the propagation must be close to pure zonal. We then use measurements or models of the zonal plasma drift and argue that the zonal wind should be in the same direction and about 15% higher. Using this estimate, along with temperature and density estimates from the MSIS computer model, we then solve the dispersion relation for gravity waves and the Doppler-shift equation simultaneously. This allows us to determine the frequency in the wind frame. A typical value for the horizontal wavelength, vertical wavelength, and period in the wind frame is 600 km, 350 km, and 25 minutes, respectively. All but two events found thus far occurred at night but the daytime cases are fascinating since the E region is expected to short out such fields. The typical gravity wave-induced vertical drift perpendicular to B in these events is a few m/s. This is sufficient to seed the Rayleigh-Taylor instability.

GWI-03 Clues to the 3D Structure of MSTID Bands Using ISR and Allsky Imaging - by Ilgin Seker

Status of First Author: Student IN poster competition PhD

Authors: Ilgin Seker (ilgins@psu.edu), Penn State University, John D. Mathews (JDMathews@psu.edu), Penn State University

Abstract: Here we report combined incoherent scatter radar (ISR) and allsky imager observations of mid-latitude F-region structures over the Arecibo Observatory in Puerto Rico. In particular, the plasma structures seen in the ISR cannot be understood fully without the all-sky images providing the context for the radar results, specifically the horizontal properties of the mesoscale structure. Here we present analysis of two specific plasma depletion events, which we prefer to call "MSTID bands". Important results on the 3D geometry of these structures were found using a specific technique. For the first time, it is shown that the MSTID bands are field-aligned. We also try to confirm our conclusions by using a 3D model based on the observations. These results give a much broader perspective on nighttime, mid-latitude F-region structure and point to new ways of interpreting these structures and how they appear in ISR results.

Instruments or Techniques for Ionospheric or Thermospheric Observation

ITI-01 Vacuum Calibrations of the Cold Cathode Gauges in HEX-2 Mission - by Lin Li

Status of First Author: Student NOT in poster competition PhD

Authors: LI, LIN (lli@clemson.edu), Lehmacher, Gerald (glehmac@clemson.edu)

Abstract: Six Cold Cathode Gauges were used to measure the neutral density profiles of the thermosphere in the HEX-2 mission launched from Poker Flat Research Range in Alaska on February 14, 2007. The gauges were calibrated in the laboratory before the flight. The results of the calibrations show small error and good reproducibility of the measurements which demonstrates the gauges are reliable in measuring the density profiles. The method of calibration will be described and the analysis and results of these calibrations will be presented.

ITI-02 Particle-In-Cell Simulation of the Incoherent Scatter Radar Spectrum - by Marcos Diaz

Status of First Author: Student IN poster competition PhD

Authors: Marcos Diaz

Abstract: A Particle-In-Cell (PIC) approach is presented and utilized to simulate Incoherent Scatter Radar (ISR) spectra. In particular, a 2D simulation is performed to a small F-region plasma volume in thermodynamic equilibrium and in absence of magnetic field. The simulation is compared to the analytical ISR spectra obtained to a plasma in thermodynamic equilibrium. The simulated ISR and the analytical ISR showed to be in agreement. Even though some plasma parameters have to be modified to limit the computational cost, the physical conclusions obtained by simulation can remain unaltered. This approach can be used to study distorted ISR spectra to obtain insights into the underlying physical phenomena.

Simulation also provides a means for studying the time evolution of spectral distortions. This could enable the development of procedures for estimating plasma parameters from distorted spectra.

ITI-03 Modeling Plasma Interactions with Satellite-Borne Instrumentation - by Jeffrey Klenzing

Status of First Author: Student IN poster competition PhD

Authors: J. H. Klenzing, G. D. Earle, R. A. Heelis

Abstract: We have developed a simulation of ion interactions with the biased grids of the Retarding Potential Analyzer (RPA), which is one of the fundamental instruments of space science. RPAs have successfully been flown on spacecraft since the late 1950's, including Sputnik III, the Viking lander, and the DMSP family of satellites. The analysis technique used in the RPA is also fundamental to the measurements made by the Ram Wind Sensor, a neutral wind anemometer to be launched as part of C/NOFS in the near future. Both instruments measure the distribution of particle flux as a function of ion energy by using biased grids as an energy filter for collected particles. In order to fit collected data to physical parameters, the interaction of charged particles with the biased grid must be studied thoroughly. We have simulated this interaction using ANSYS, a multiphysics software tool. Perturbations to the Whipple RPA equation due to non-uniform potential will be discussed with the intent of developing quantitative corrections to inferred parameters, such as velocity and temperature.

ITI-04 A 1083 nm lidar for observations of temperature in the upper thermosphere - by Chad G. Carlson

Status of First Author: Student IN poster competition PhD

Authors: C.G. Carlson, G.R. Swenson, P.D. Dragic, and L. Waldrop, Dept. of Electrical and Computer Engineering, University of Illinois at Urbana-Champaign

Abstract: Although metastable helium (He), which sparsely populates the upper thermosphere and lower exosphere, was first identified as a candidate target for resonance fluorescent lidars by Gerrard et. al. in 1997, technological limitations ten years ago hindered the pursuit of thermospheric lidar capability. However, recent developments in semiconductor lasers, high power rare-earth-doped fiber amplifiers, and compound semiconductor photon detectors have placed the reality of a He resonance fluorescence lidar capability firmly within reach. This poster details the development and deployment of a high power Doppler narrowband lidar transmitter at 1083 nm at the University of Illinois at Urbana-Champaign for making detailed temperature measurements in the upper thermosphere from 300-700 km.

ITI-05 Remote O(3P) Sensing by Ionospheric Excitation (ROSIE) - by Konstantinos Kalogerakis

Status of First Author: Non-student

Authors: K. S. Kalogerakis [1], T. G. Slanger [1], and E. A. Kendall [2], [1] Molecular Physics Laboratory, SRI International [2] Center for Geospace Studies, SRI International

Abstract: The principal optical observable resulting from ionospheric modification (IM) experiments is the oxygen red line at 630 nm, originating with the O(1D - 3P) transition. Because the O(1D) atom has a radiative lifetime of 110 s, it is very sensitive to collisional quenching, and a decay faster than the radiative rate can be attributed to collisions with atmospheric particles. In contrast to the common practice of ignoring O-atoms in interpreting such observations in the past, our recent experimental studies on the relaxation of O(1D) by O(3P) have revealed the dominant role oxygen atoms play in controlling the lifetime of O(1D) at altitudes relevant to IM experiments. Using the most up-to-date rate coefficients for collisional relaxation of O(1D) by O, N₂, and O₂, it is now possible to analyze reliably the red line decays observed in IM experiments and thus probe the local O-atom density in the ionosphere. In this manner, we can demonstrate an innovative approach to remotely probe O-atoms at the altitudes relevant to IM experiments, test the current models for O-atom density in the ionosphere, and study its temporal, seasonal, altitude and spatial variation in the vicinity of heating facilities.

In the experiments, molecular oxygen is photodissociated to O(1D) and O(3P) atoms by the 157 nm output of a fluorine laser. The temporal evolution of the O(1D) concentration is monitored by detection of the 630-nm emission. Our current laboratory results indicate that O(1D) relaxation by O(3P) atoms is very efficient. We discuss the relevance to atmospheric observations and ionospheric heating experiments.

Over the last 35 years a number of IM experiments have been reported. With knowledge of the O(1D) + O(3P) rate coefficient, we are able to compare the results of these studies with atmospheric composition models, realizing that the energy is absorbed over some altitude range. We report a preliminary analysis of data that have been accumulated from a number of IM sites to show that it is generally possible to map out overhead O(3P) by this method and present plans for more detailed collaborative studies in the future.

The laboratory experiments relevant to this presentation were supported by the NSF Aeronomy Program.

ITI-06 The influence of high-energy electron precipitation on the midlatitude nighttime D region - by Feng Han

Status of First Author: Student IN poster competition Masters

Authors: Feng Han, feng.han@duke.edu ,Steven A. Cummer, cummer@ee.duke.edu

Abstract: Very low frequency (VLF, 3-30 kHz) electromagnetic waves generated by lightning discharges and propagating for long distances in the Earth-ionosphere waveguide can be used to measure the average electron density profile of the lower ionosphere along the wave propagation path. This capability enables frequent if not continuous monitoring of the D region electron density profile over geographically large regions, which are measurements that are essentially impossible by other means. Significant temporal variability of the nighttime D region is well known, and we aim to apply this approach to better understand the sources of this variability. We report the analysis of data recorded between 1 June to 31 August 2005 and 0600 to 0900 UT (local night) from lightning that was 300–1000 km away from our sensors at Duke University. By comparing 20 typical observed VLF spheric spectra with corresponding simulated results from a 2D FDTD model, we extracted the two-parameter exponential electron density profile for each measurement. Using the flux of 100–300 keV electrons measured by NOAA-18 satellite in the vicinity of the ionospheric measurement, we investigate the detailed influence of high-energy particle precipitation on the D region ionospheric electron density profile.

ITI-07 Improved electron density profile estimation at Jicamarca - by Fabiano S Rodrigues

Status of First Author: Student IN poster competition PhD

Authors: Fabiano S Rodrigues, Cornell University,,Michael J Nicolls, SRI International, David L Hysell, Cornell University

Abstract: We report improvements in the estimation of electron density profiles at Jicamarca. We used full incoherent scatter (IS) theory to calculate the total radar cross section and applied the results in the correction of power profiles so that they better

represent the height variation of the ionospheric electron density. This correction is necessary when the electron-to-ion temperature ratio is greater than 1. Power, Faraday rotation and temperatures are provided by the double-pulse experiment. We compared the corrected power profiles with Faraday rotation profiles measured simultaneously. They agree within their uncertainties.

ITI-08 Recent observations of the proton gyroresonance at Jicamarca - by Fabiano S Rodrigues

Status of First Author: Student NOT in poster competition PhD

Authors: Fabiano S Rodrigues, Cornell University, Michael J Nicolls, SRI International, Ronald Woodman, Instituto Geofisico del Peru, David L Hysell, Cornell University, Jorge L Chau, Jicamarca Radio Observatory, Sixto Gonzalez, Arecibo Observatory

Abstract: We will be reporting recent measurements of the proton gyroresonance in the topside ionosphere over Jicamarca. We were able to measure the first peak of the proton gyroresonance in the IS autocorrelation function at night around 700 km for a few hours on October 11 and 12, 2006. Using full incoherent scatter theory including Coulomb collisions we inferred least-squares best estimates of the temperature (assuming $T_e = T_i$) and H^+ fraction from the observations. Our results indicate that observations of the gyroresonance might be useful for parameter estimation in the topside equatorial ionosphere during periods of reduced clutter from coherent echoes.

ITI-09 Transmitting Antennas for Modern Ionosondes - by Bill Wright – presented by Nick Zabolin

Status of First Author: Non-student

Authors: J. W. Wright and N. A. Zabolin (University of Colorado at Boulder, USA)

Abstract: This "nuts and bolts" topic is worth brief attention by the aeronomic community, because the modern ionosonde (as exemplified by Dynasonde principles of flexibility and diversity of data acquisition, precision of measurements, real-time performance, objective error estimates and reasonable cost) is becoming recognized as the most essential component of an atmospheric-science observatory. The transmitting antenna will define many of the site requirements and it may limit the performance of the instrument.

We use the familiar "NEC-2" antenna modeling program as wrapped in 'MultiNEC'© for convenient design input, control and graphic output. Our own software generates (at present) seven characteristic antenna types: Delta, Rhombic, Zig-zag Log Periodic, 'Bent ZZLPA', Conical Log Spiral, Planar Log Spiral and 'Cobra' designs. All relevant design parameters for each type may be freely chosen to define the antenna in straight-wire segments. The performances of various practical designs are characterized by frequency-dependent patterns, standing-wave ratios (SWR) and polarization characteristics, in addition to cost and construction considerations.

Special attention is given to the problem of maintaining useful performance at radio frequencies well below the nominal design limit; in this frequency range most antennas will display large SWR values which may not be tolerated by modern solid-state power amplifiers.

ITI-10 Line-of-sight Doppler and vector velocity relationships for HF sounding in the equatorial ionosphere - by Nick Zabolin

Status of First Author: Non-student

Authors: N.A. Zabolin, J.W. Wright (University of Colorado at Boulder, USA) and G.A. Zhabankov (Institute of Physics, Southern Federal University, Russia)

Abstract: We present results of numerical simulation of line-of-sight Doppler measurements and vector velocity determinations based on them, for the equatorial ionospheric F region. A typical situation is modeled where the ionospheric E region is filled with small-scale irregularities originated by equatorial electrojet, and is moving at a velocity not coinciding with the F region velocity. Irregularities in ionospheric layers are modeled by small-scale (~1-2 km) wave-like structures, and the movements of the layers are modeled by movements of these structures. Parameters of the sounding radio signals are determined through a procedure of multiple numerical solving of the extended ray tracing equation set.

It is shown that when F region vector velocities are calculated from the line-of-sight Doppler values, and are attributed to the reflection level according to the standard procedure, these demonstrate a significant bias if a differently-moving E-region is present. The magnitude of this bias depends not only on the E-F vector velocity difference, but also on the amplitude of the E-region irregularities.

This result is in qualitative and quantitative agreement with the recent experimental observations published by Woodman and Chau, suggesting necessity of a special inversion procedure for obtaining the vector velocity, that treats properly the differential motion of ionospheric layers.

ITI-11 Investigation of a new incoherent scatter coding technique for F-region observations at the Arecibo observatory - by Romina Nikoukar

Status of First Author: Student IN poster competition PhD

Authors: Romina Nikoukar, Nikoukar@uiuc.edu, Farzad Kamalabadi, farzadk@uiuc.edu, Michael Sulzer, msulzer@naic.edu, Erhan Kudeki, erhan@uiuc.edu, Sixto Gonzalez, sixto@naic.edu

Abstract: In this work, we describe a new multiple radar autocorrelation function (MRACF) experiment that was conducted at the Arecibo observatory in July 2006, and we present the ionospheric parameter estimation results obtained from this set of observations. The main goal of this experiment was to compare the performances of the long pulse modulation and the simplex coding scheme. The simplex modulation technique proposed by Nikoukar et al. [2007] consists of transmission of two amplitude modulated pulses derived from the so-called Simplex matrix. This coding technique is primarily designed to result in a more accurate estimation of ionospheric parameters for high signal-to-noise ratio (SNR) situations due to the following reasons: this technique provides a more uniform distribution of the number of contributing altitudes in each autocorrelation function (ACF) lag estimate while it yields less correlation between lag-estimate errors. To compare the performances of the two modulation techniques, we modified the traditional mode of MRACF to alternate between the simple long pulse and the two simplex codes with a pulse repetition period of 10 ms. Moreover, in order to provide a ground truth for our estimation results, we further utilized the power profile mode to measure the electron density profile with a fine range resolution (600 m). The inversion analysis of the simplex-code data shows a 40% reduction in the parameter error variances along with the reduced oscillatory artifacts in the altitude profiles of the extracted parameters often associated with the long-pulse modulation.

ITI-12 Focal Phased Array Prototype for the Arecibo Telescope - by Eliana Nossa

Status of First Author: Student IN poster competition PhD

Authors: Eliana Nossa (en45@cornell.edu) and German Cortes-Medellin (gcortes@astro.cornell.edu)

Abstract: A focal phased array is an array of antennas connected through beamformer boards. The resultant antenna beam can be electronically controlled to change instantaneously the direction of the beam and to create multiple beam operations. The result presented in the poster contemplates the design of Vivaldi antennas with novel modifications and the design and fabrication of the analog beam former, operating in a microwave range of frequencies, with a bandwidth of 2:1 and final gain of 20dB. The criteria used throughout the design were to optimize the bandwidth, minimize the return losses and the coupling, and maximize the gain and signal-to-noise ratio of the beam-former.

New Instrumentation

NEW-01 Ionospheric annual variations observed by the COSMIC radio occultation technique and simulated by the TIEGCM - by Zhen Zeng

Status of First Author: Non-student

Authors: Zhen Zeng (HAO/COSMIC, zzeng@ucar.edu), Alan Burns (HAO, aburns@ucar.edu), Wenbing Wang (HAO, wbwang@ucar.edu), Jiuhou Lei (HAO, leijh@hao.ucar.edu), Stan Solomon (HAO, stans@ucar.edu), Stig Syndergaard (COSMIC, ssy@ucar.edu), Liying Qian (HAO, lqian@ucar.edu), and Ying-Hwa Kuo (COSMIC, kuo@ucar.edu)

Abstract: The F2-layer annual asymmetry is a well-observed ionospheric anomaly that has been widely discussed for several decades, but the mechanisms of the annual asymmetry are still unexplained. This study looks at global variations of this annual asymmetry in NmF2 observed from one-year of COSMIC ionospheric radio occultation (IRO) measurements (2006-2007). The IRO observations show that there is a strong NmF2 annual asymmetry that has significant longitudinal and local time variations. A strong peak of the asymmetry occurs at about 14-16 LT and another one at midnight, both occur at around 20 degrees latitude. Numerical simulations using the Thermosphere-Ionosphere Electrodynamics Global Circulation Model (TIEGCM) are in very good agreement with these observations. The modeled NmF2 annual asymmetry has the same magnitude, and same semi-diurnal and longitudinal variations as those in the observations. TIEGCM simulations show that changes in solar radiation between December and June and the displacement of geomagnetic poles from geographic poles are the two primary reasons for these annual asymmetries and their associated longitudinal and local time variations. Other factors, such as lower altitude tides and high latitude energy inputs, are also partly responsible for this asymmetry.

NEW-02 Reconstructing the Ionosphere for the Long Wavelength Array - by Christopher Watts

Status of First Author: Non-student

Authors: Christopher Watts (UNM), on behalf of the LWA project

Abstract: The Long Wavelength Array (LWA, lwa.unm.edu) is a new telescope/interferometer facility being established to do astrophysical observations in the frequency range 10 MHz to 90 MHz. As such, measurements will be strongly affected by the ionosphere. In fact, part of the LWA mandate is to make highly precise measurements of the ionosphere. The work will require a combination of active and passive measurements, detailed modeling and improvement of existing telescope “self-calibration” techniques. This presentation will give an overview of the requirements, with the aim of stimulating discussion in the ionospheric community on how to address these issues.

NEW-03 Drag and Atmospheric Neutral Density Explorer (D A N D E) - by Scott E Palo

Status of First Author: Non-student

Authors: S. Palo(1), M. Pilinski(2), M. Grusin(2), C. Koehler(2), J. Forbes(1), (1) Aerospace Engineering Sciences, University of Colorado, Boulder, CO 80309, (2) Colorado Space Grant Consortium, University of Colorado, Boulder, CO 80309

Abstract: DANDE is a small satellite (50 kg class) being designed at the University of Colorado, Boulder to study neutral density, winds, composition, and coefficient of drag variations in the thermosphere. Three instruments on the spacecraft as well as ground tracking will provide this in-situ data over a three month period as the orbit is lowered by drag from 350 to 100 km. DANDE will include a miniature neutral-mass spectrometer, ionization pressure gauges, and commercial off-the shelf accelerometers. The neutral mass spectrometer will make number density measurements of molecular nitrogen and atomic oxygen in the ram direction. The pressure gauges will point in the cross-track direction to provide measurements of neutral winds. Accelerometer measurements will be used to deduce atmospheric density as both the mass and cross-sectional area of this spherical spacecraft are fixed. Accelerometer derived density and spectrometer derived density measurements can be combined on the ground to deduce in-track winds. This is because accelerometer measurements are proportional to velocity squared while spectrometer measurements are proportional to velocity. This low-cost spacecraft is being designed and built by students as a means of providing affordable, continuous, and distributed data in the future. The desired launch date is planned for 2009 and 2011 during solar maximum.

NEW-04 ISIS multi-antenna operation and calibration - by Zachary Berkowitz

Status of First Author: Student NOT in poster competition Masters

Authors: Berkowitz, Zachary; Sahr, John (University of Washington); Lind, Frank (MIT Haystack)

Abstract: The Intercepted Signals for Ionospheric Science (ISIS) project (Lind, MIT Haystack) project comprises a synchronous network of digital receivers with six RF ports. The ISIS receivers are far more capable than the digital receivers which make up the Manastash Ridge Radar; we are in the process of transferring to these new receivers. Among other things, the new receivers will permit absolute angle of arrival to be estimated in interferometric observation of auroral irregularities and meteor trails. In addition we will be able to observe satellite beacons for scintillation studies, and VLF transmissions for D Region absorption. In this report we describe our initial efforts to implement and calibrate a six antenna system for the passive radar reference system at

the University of Washington. We are especially interested in developing calibration methods which can be performed remotely without special test equipment. It is expected that the receivers will be in continuous operation and in remote locations which discourage calibration strategies which require intervention.

NEW-05 Optimizations for Digital Radar Receivers - by Matthew Sunderland

Status of First Author: Student NOT in poster competition Undergraduate

Authors: Matthew Sunderland, Tamara Hall, Sixto Gonzalez, Julio Urbina

Abstract: Various techniques for improving the performance of a digital radar receiver are presented. Direct digital frequency synthesis systems enjoy benefits of the digital domain such as replication, flexibility, and compactness at the cost of finite precision arithmetic. Methods such as phase dithering, Taylor Series approximations, and amplitude-difference storage are employed to minimize the effects of finite precision. Focus is aimed at limiting the presence of spectral impurities and improving the signal-to-noise ratio while minimizing logic resources.

NEW-06 Distributed Observatory in South America of Ionospheric Measurements and Current Status - by Elizabeth Silvestre

Status of First Author: Non-student PhD

Authors: 1.Elizabeth Silvestre, Radio Observatorio de Jicamarca - Instituto Geofisico del Peru. 2.Cesar Valladares Institute for Scientific Research' Boston College – USA, 3. Jorge Chau, Radio Observatorio de Jicamarca - Instituto Geofisico del Peru - Lima

Abstract: In this work we present the current status of the LISN (Low-latitude Ionospheric Sensor Network) . LISN is a multi-instrument (GPSs, Ionosondes and magnetometers) and multi-institutional project lead by Boston College and Jicamarca incoherent scatter radar (ISR). The geophysical instruments are being installed within South America around the magnetic meridian 70°W, with the purpose of studying and forecast the ionospheric equatorial phenomena. Special emphasis will be placed in the dynamics and the photochemical energy transport processes in the low, middle and upper atmosphere. LISN will work continuously and in near real time. Data from all the instruments will be sent to IGP (Instituto Geofisico del Peru) headquarters, who is in charge of the operations, database as well as data quality and control.

Index

Alken, Patrick, 1

Bass, Elizabeth, 12
Berkowitz, Zachar, 20
Bhaneja, Preeti, 4
Briczinski, Stanley, 11
Bryson, Gwendolyn, 13

Capozzi, Stephen, 10
Carlson, Chad, 16
Chapagain, Narayan, 2

Danielides, Michael, 6
Deng, Yue, 8
Diaz, Marcos, 16

Eastes, Richard, 9
Emery, Barbara, 6

Fang, Tzu-Wei, 1
Fang, Xiaohua, 7
Fedrizzi, Mariangel, 5
Fentzke, Jonathan, 12

Garner, Trevor, 2

Han, Feng, 17
Hei, Matthew, 1
Heinselman, Craig, 10

Ilma, Ronald, 2

Jackel, Brian, 8

Kalogerakis, Konstantinos, 17
Kim, Yong Ha, 3
Klenzing, Jeffrey, 16
Kwak, Young-Sil, 7

Li, Lin, 15
Line, Michael, 12
Livneh, Dorey, 14

Malhotra, Akshay, 11
Martinis, Carlos, 14
Michell, Robert, 11
Mierkiewicz, Edwin, 4

Narvaez, Clara, 8
Nikoukar, Romina, 19
Nishioka, Michi, 9
Nossa, Eliana, 19
Nossal, Susan, 3

Pacheco, Edgardo, 2
Palo, Scott, 20
Parris, Richard, 13
Pawlowski, David, 3

Rodrigues, Fabiano, 17, 18

Seker, Ilgin, 15
Shim, Ja Soon, 5
Silvestre, Elizabeth, 21
Spaleta, Jeffrey, 13
Sunderland, Matthew, 21

Taylor, Brandon, 8
Twork, Greg, 13

Varney, Roger, 15

Waldrop, Lara, 4
Watts, Christopher, 20
Wright, Bill, 18

Yokoyama, Tatsuhiro, 14

Zabotin, Nick, 18
Zeng, Zhen, 19
Zettergren, Matthew, 10
Zou, Shasha, 7